Journal of Power Sources, 43–44 (1993) 195–208

Ambient temperature rechargeable polymer-electrolyte batteries

K. M. Abraham and M. Alamgir
EIC Laboratories, Inc., 111 Downey Street, Norwood, MA 02062 (USA)

Abstract

Li^+-conductive solid polymer electrolytes with room temperature conductivities of about 2×10^{-3} Ω^{-1} cm^{-1} have been developed. Solid-state $Li/LiMn_2O_4$ and $C/LiNiO_2$ batteries employing these electrolytes have been fabricated and tested. These batteries have shown room temperature performance reminiscent of their liquid electrolyte counterparts.

Introduction

The development of ambient temperature rechargeable polymer-electrolyte batteries has remained a formidable challenge. This challenge stems primarily from the requirements of polymer electrolytes for such batteries. In addition to its role as an ion-transporting medium, the polymer electrolyte must function as a separator in the battery. That means that polymer electrolytes suitable for ambient temperature batteries must exhibit good dimensional stability while possessing all the characteristics of traditional nonaqueous electrolytes including a conductivity of $>10^{-3}$ Ω^{-1} cm^{-1} at 25 °C, a value typically found in the realm of liquid electrolytes. Good dimensional stability means that it must be possible to process the polymer electrolyte into free-standing thin films having mechanical strength adequate for withstanding the physical dynamics of the electrodes during cycling of secondary lithium batteries. In this respect, the mechanical strength of polymer electrolytes should be comparable to that of conventional, nonaqueous liquid electrolyte battery separators such as porous polyethylene and polypropylene membranes having typical thicknesses of 0.0025 to 0.005 cm. On the other hand, to expect an ionic conductivity similar to that of highly conductive liquid electrolytes and a dimensional stability reminiscent of solids in the same polymer electrolyte is to expect the coexistence of two properties which are probably mutually exclusive, especially in view of the fact that the mechanism by which ions are transported in polymer electrolytes is not significantly different from that involved in liquid electrolytes. Indeed, it has been necessary to pursue innovative approaches in order to develop polymer electrolytes having room temperature conductivities of the order of 10^{-3} Ω^{-1} cm^{-1} [1–5].

Ambient temperature polymer electrolytes

Classical polymer electrolytes, composed of Li salt (e.g., $LiClO_4$, $LiBF_4$, $LiCF_3SO_3$, etc.) complexes of poly(olefin oxide)s, $\{RCRCH–CH_2O\}_n$ in which R=H for

0378-7753/93/$6.00

poly(ethylene oxide) (PEO) and R=CH_3 for poly(propylene oxide) (PPO) are solids at room temperature. Consequently, their room temperature conductivity is very low, being of the order of 10^{-9}–10^{-8} Ω^{-1} cm^{-1}.

The ionic conductivity, σ, of an electrolyte is given by the product of the concentration of ionic charge carriers and their mobility:

$$\sigma = \sum_i n_i z_i \mu_i \tag{1}$$

In eqn. (1), z_i is the ionic charge, n_i is the number of charge carriers and μ_i is the ionic mobility. High conductivity in an electrolyte is obtained by increasing both the mobility and concentration of ionic charge carriers.

When different polymer electrolytes are derived from the same family of polymer hosts, such as the polyethers, the permittivity of the medium does not change significantly from one host to the other. The consequence of this for polyether-based electrolytes is that the concentration of the ionic charge carriers remains more or less the same irrespective of the host. Barring a major enhancement of the permittivity of the polymer host, the room temperature conductivity of polymer electrolytes can be appreciably increased only by increasing the mobility of the ionic charge carriers. This may be accomplished by providing a fluid environment for ionic motion in the polymer matrix. Indeed, the coupling of high ionic conductivity to polymer fluidity is reflected in the description of the temperature dependence of ionic conductivity of polymer electrolytes by the Vogel–Tamman–Fulcher (VTF) equation:

$$\sigma = AT^{-1/2}\, e^{-B/(T-T_0)} \tag{2}$$

In this equation, σ is the conductivity, A is a constant proportional to the number of carrier ions, B is a constant related to energy, and T_0 is the temperature at which the configuration entropy of the polymer becomes zero and is close to the glass transition temperature (T_g). The VTF equation fits conductivity rather well over a broad temperature range extending from T_g to about $T_g + 100$ K. Equation (2) is an adaption of the relationship developed to explain the temperature dependence of such polymer properties as viscosity, dielectric relaxation time and magnetic relaxation rate. The VTF equation relating viscosity and T is:

$$\eta^{-1} T = A\, e^{-B/(T-T_0)} \tag{3}$$

The fact that eqn. (2) can be applied to conductivity implies that, as with viscosity, ionic conductivity in polymers is strongly coupled to the flow behavior of the polymer. Lower T_g and a fully amorphous morphology produces greater polymer flow and ionic diffusivity. That is to say high ionic conductivity is obtained in amorphous polymers having highly flexible backbones and low glass-transition temperatures. Electrolytes derived from poly[bis-((methoxyethoxy)ethoxy)phosphazene], MEEP, illustrate this behavior rather well. MEEP–$(LiX)_{0.25}$, where LiX = $LiBF_4$, $LiCF_3SO_3$, $LiClO_4$, $LiAsF_6$, etc., however are glutinous electrolytes with a tendency to flow even under mild compression and they cannot be cast as free-standing films [1]. For a battery technologist the question is how to obtain polymer electrolytes with good mechanical strength while maintaining an ionic environment of high fluidity in it.

Dimensionally-stable conventional electrolytes with high room temperature conductivity

Here, electrolytes derived from long-chain polymer hosts are called conventional electrolytes. A convenient way of preparing electrolytes with good dimensional stability and high conductivity is to form Li salt complexes of polymer composites, blends of

two or more polymers. In the composite electrolyte of interest here, a relatively fluid polymer host such as MEEP facilitates ionic transport while a rigid polymer such as poly(ethylene oxide) (PEO), poly[(ethylene glycol)diacrylate] (PEGDA) or poly(vinyl pyrrolidinone) (PVP) imparts mechanical strength to the film [1, 2]. The structures of these polymers are shown below. Composite electrolytes which we have prepared include xMEEP/yPEO–(LiX)$_n$, xMEEP/yPPO–(LiX)$_n$, xMEEP/yPEGDA–(LiX)$_n$ and xMEEP/yPVP–(LiX)$_n$, where x and y are the wt.% of MEEP and the rigid polymer, respectively, and n is the mole ratio of the Li salt to the complexing oxygens in the polymer host. Lithium salt complexes of MEEP/PEO and MEEP/PPO composites were made by mixing the components in appropriate solvents followed by evaporation of the solvent. The MEEP/PVP and MEEP/PEGDA composite electrolytes were made by radiation polymerization of the monomers of PVP or PEGDA in the presence of MEEP–(LiX)$_n$.

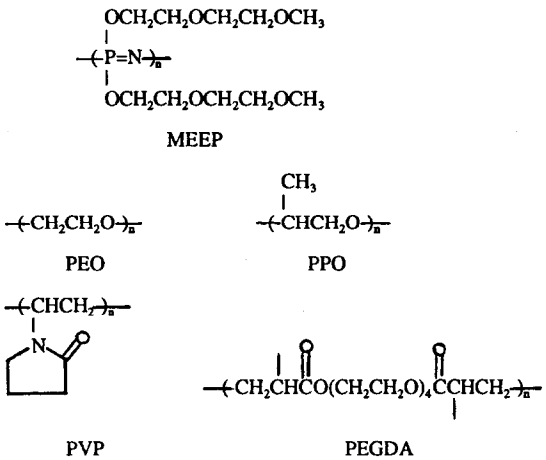

The conductivities of a number of dimensionally-stable MEEP-based composite electrolytes are presented in Table 1. The composite electrolytes have slightly lower conductivity than that of neat MEEP–(LiX)$_n$. However, they have excellent dimensional stability and can be prepared as free-standing films suitable for use as separators in polymer-electrolyte batteries. The data in Table 1 suggest that the conductivity of these materials is influenced by the nature of the anion in the Li salt; the highest conductivity is exhibited by complexes of $LiN(CF_3SO_2)_2$. The exceptionally high conductivity of complexes containing this salt has been attributed to its plasticizing effect. Alternatively, their higher conductivity may be due to a greater charge-carrier concentration coming from the fact the large imide anion discourages ion-pair formation. Electrolyte no. 8 in Table 1 is one of the highest conductive, dimensionally-stable, conventional polymer electrolyte presently known. Since a polymer host with greater fluidity that exhibited by MEEP would have poorer dimensional stability, it is probably not unreasonable to conclude that a conductivity of about 10^{-4} Ω^{-1} cm^{-1} at room temperature (a value in the realm of the conductivity of electrolyte no. 8 in Table 1) perhaps represents the highest that can be achieved in a polymer electrolyte derived from a long-chain polymer host. These electrolytes are probably more appropriate for applications in the vicinity of about 50 °C than at room temperature.

TABLE 1

Conductivity of MEEP-based polymer electrolytes

Electrolyte	Conductivity (Ω^{-1} cm^{-1})		
	20	50	80 (°C)
1 MEEP–$(LiClO_4)_{0.25}$	1.7×10^{-5}	7.0×10^{-5}	
2 MEEP–$(LiBF_4)_{0.25}$	1.5×10^{-5}	5.0×10^{-5}	1.4×10^{-4}
3 MEEP–$(LiCF_3SO_3)_{0.25}$	1.5×10^{-5}	3.8×10^{-5}	
4 MEEP–$[LiN(CF_3SO_2)_2]_{0.13}$	6.5×10^{-5}	1.6×10^{-4}	
5 55[a]MEEP/45 PEO–$(LiClO_4)_{0.13}$	1.3×10^{-6}	9.0×10^{-6}	2.7×10^{-4}
6 55[a]MEEP/45 PEO–$(LiBF_4)_{0.13}$	2.4×10^{-6}	2.0×10^{-5}	3.5×10^{-4}
7 55[a]MEEP/45 PEO–$(LiCF_3SO_3)_{0.13}$	1.0×10^{-6}	6.0×10^{-6}	3.5×10^{-5}
8 55[a]MEEP/45 PEO–$[LiN(CF_3SO_2)_2]_{0.13}$	6.7×10^{-5}	1.2×10^{-4}	
9 55[a]MEEP/45 PEO–$(LiAsF_6)_{0.13}$	1.9×10^{-7}	1.2×10^{-6}	1.5×10^{-5}
10 87[a]MEEP/13 PEGDA–$(LiClO_4)_{0.13}$	1.2×10^{-6}	7.2×10^{-6}	3.8×10^{-4}
11 87[a]MEEP/13 PVP–$(LiClO_4)_{0.13}$	4.0×10^{-6}	2.3×10^{-5}	4.0×10^{-4}
12 55[a]MEEP/45 PEO–$(LiBF_4)_{0.13}$	4.0×10^{-7}	6.3×10^{-6}	
13 PEO–$(LiClO_4)_{0.13}$ [b]	4.0×10^{-9}	6.4×10^{-7}	2.5×10^{-5}

[a]Dimensionally-stable composite electrolytes; all ratios are in wt.%.
[b]Given for comparison.

Nonconventional electrolytes with good dimensional stability and high room temperature conductivity

Dimensionally-stable polymer electrolytes with conductivities of the order of 10^{-3} Ω^{-1} cm^{-1} at room temperature can be prepared according to a procedure which may be viewed as an extension of the composite concept. In these, at least one component of the composite host is a low volatile liquid with high dielectric constant. The polyacrylonitrile (PAN)-based electrolytes we have recently prepared [1, 3] belong to this class of materials. They are obtained by immobilizing Li salt solvates of a mixture of propylene carbonate (PC) and ethylene carbonate (EC) in the PAN polymer network. The structures of EC, PC and PAN are shown below. The room temperature conductivities

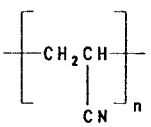

PAN

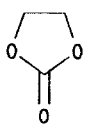

EC

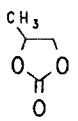

PC

of a number of these electrolytes are listed in Table 2. They show a conductivity in the range of $1–2\times10^{-3}$ Ω^{-1} cm^{-1}. When viewed from the perspective of eqn. (1), the high ionic conductivity of these electrolytes can be seen as the result of both higher concentration and greater mobility of the charge carriers. We have found that other polymer networks such as PEGDA and PVP can also be used [2–4]. The data in Table 2 indicate that the room temperature conductivity of these electrolytes depends on the nature of the Li salt (compare electrolytes nos. 4–8), the nature of the polymer network (compare electrolytes nos. 1 and 10–12) and the ratio of the polar liquids (compare electrolytes nos. 1 and 3). That means that the conductivities of these types of electrolytes can be tailored by judiciously selecting their components. Table 3 lists

TABLE 2

Conductivities of PAN-, PVP- and PEGDA-[a]based electrolytes at 25 °C

Electrolytes[b]	Conductivity at 20 °C, Ω^{-1} cm^{-1}
1. 21% PAN/38%[b] EC/33% PC/8% $LiClO_4$	1.7×10^{-3}
2. 16 PAN/62 EC/13 PC/1 PEGDA/8 $LiClO_4$	1.2×10^{-3}
3. 16 PAN/68 PC/16 $LiClO_4$	8.6×10^{-4}
4. 20.6 PAN/61 EC/13.2 PC/5.2 $LiCF_3SO_3$	1.1×10^{-3}
5. 20.6 PAN/61 EC/13.2 PC/5.2 $LiBF_4$	0.3×10^{-3}
6. 20.6 PAN/61 EC/13.2 PC/5.2 $LiAsF_6$	0.8×10^{-3}
7. 17 PAN/43 EC/37 PC/3 $LiN(SO_2CF_3)_2$	1.6×10^{-3}
8. 17 PAN/64 EC/14 PC/5 $LiN(SO_2CF_3)_2$	1.8×10^{-3}
9. 3 PEGDA/68 EC/15 PC/14 $LiClO_4$	4.0×10^{-3}
10. 27 PVP/24 EC/21 PC/10 Tetraglyme/18 $LiClO_4$	8.0×10^{-4}
11. 25 PVP/35 EC/30 PC/10 $LiCF_3SO_3$	4.0×10^{-4}
12. 32 PVP/31 EC/26 PC/11 $LiCF_3SO_3$	2.4×10^{-4}
13. 35 PVP/54 PC/11 $LiCF_3SO_3$	1.5×10^{-4}

[a]PAN: polyacrylonitrile, PVP: poly(vinyl pyrrolidinone), PEGDA: poly[(tetraethylene glycol) diacrylate], EC: ethylene carbonate, PC:propylene carbonate.
[b]Compositions of electrolytes are in mol%.

TABLE 3

PAN-based electrolytes with improved low temperature conductivities[a]

Electrolyte[b]	Conductivity (Ω^{-1} cm^{-1}) 10^{-3}			
	−40	−20	0	20 (°C)
21PAN–33PC–38BL–8$LiClO_4$	0.30	0.98	1.94	3.71
21PAN–33PC–10EC–18BL–10NMP–8$LiClO_4$	0.20	0.74	1.93	2.57
21PAN–33PC–20EC–18BL–8$LiAsF_6$	0.28	1.15	1.73	3.87

[a]PAN: polyacrylonitrile, PC: propylene carbonate, BL: butyrolactone, EC: ethylene carbonate, and NMP: N-methylpyrrolidinone.
[b]All ratios are mol%.

electrolytes with improved low temperature conductivities we have prepared utilizing this principle. They have conductivities of about 3×10^{-3} Ω^{-1} cm^{-1} at 20 °C and about 10^{-3} Ω^{-1} cm^{-1} at −20 °C, values in the realm of traditional nonaqueous liquid electrolytes.

The significantly higher ambient temperature conductivity of PAN-based electrolytes compared with conventional electrolytes derived from long-chain polymer hosts is readily discernible from the data presented in Fig. 1. The nonconventional electrolytes described here exhibit high ionic conductivities at room temperature because of the presence of an appreciable amount of liquid component. However, they should be seen as a special group of materials in their own right. They are amorphous solids with good dimensional stability and are suitable for use as electrolyte-cum-separators in batteries. Their discovery has enabled us to fabricate and test solid-state Li and

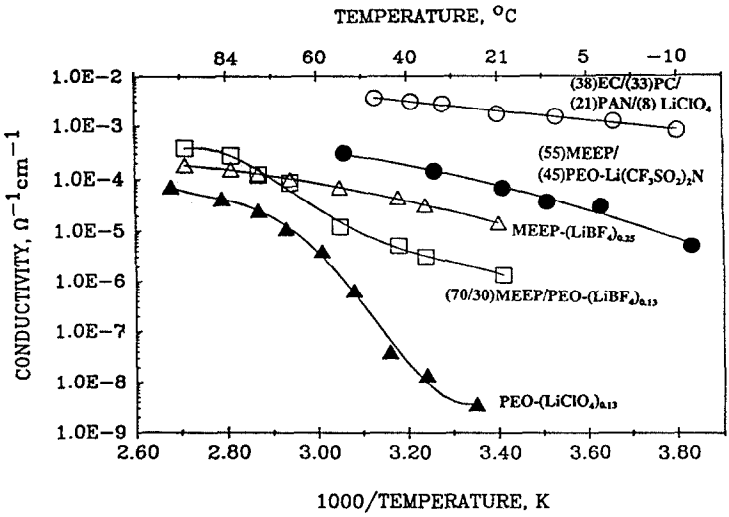

Fig. 1. A comparison of the conductivities of some polymer electrolytes.

Li ion batteries whose discharge rate capabilities approach that of their liquid electrolyte counterparts.

Ambient temperature polymer-electrolyte batteries

We have fabricated and tested solid-state cells containing both MEEP-based and PAN-based electrolytes. The results obtained from the MEEP-based Li/TiS_2 cells have been published [2, 6]. Those cells showed excellent rechargeability with one cell exceeding two hundred full depth-of-discharge cycles. The results have demonstrated the exceptional stability of the Li/MEEP interface. Recently, rechargeable $LiMn_2O_4$, C/$LiNiO_2$ and C/$LiCoO_2$ cells with PAN-based electrolytes have been built and tested. These cells were constructed from laminates of polymer electrolyte, composite cathode, and Li metal or composite carbon anode. The Li anodes were composed of 25 μm thick Li foil, pressed on a Cu substrate, obtained from Cypress Foote Company. The polymer-electrolyte laminates had thicknesses between 50 and 100 μm. The composite cathode or the carbon anode laminate consisted of a mixture of the active material, the polymer electrolyte and a binder, coated on a metal foil current collector. The cells had about 10 cm^2 electrode area and a theoretical capacity of approximately 10 mA h. A schematic representation of the cell is presented in Fig. 2.

Lithium–manganese dioxide cells

The capacity/rate behavior of a Li/PAN–EC–PC–$LiAsF_6$/$LiMn_2O_4$ cell at three different temperatures is displayed in Fig. 3. The theoretical capacity of the cell was approximately 7 mA h. Discharge rates as fast as the $C/2$ rate were possible with good cathode utilization. This performance is typical of liquid electrolyte-based secondary Li batteries. The room temperature cycling behavior of another Li/$LiMn_2O_4$ cell is presented in Fig. 4. The cell has approximately the same theoretical capacity as the one in Fig. 3. The cell has exceeded 200 cycles.

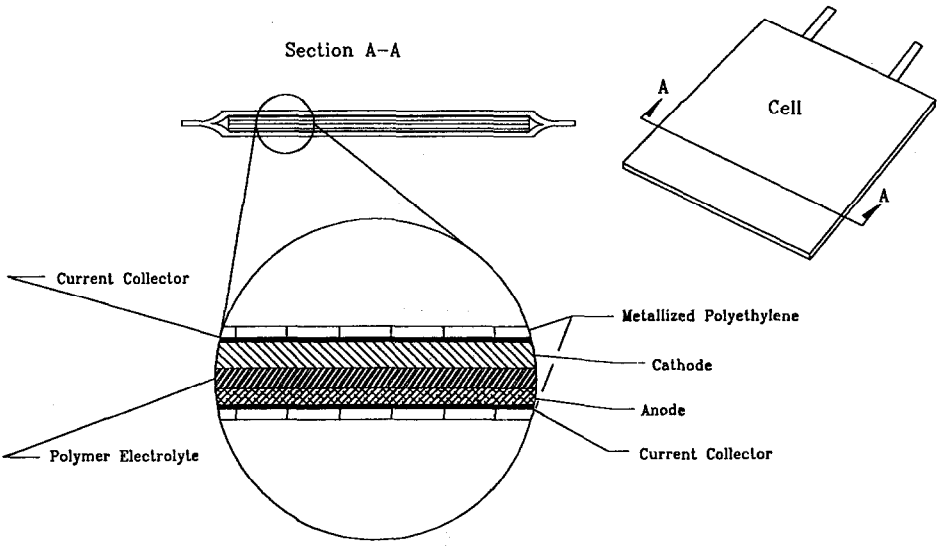

Fig. 2. Schematic representation of sealed solid-state cells.

The lithiated manganese dioxide ($Li_xMn_2O_4$) can also be used as a four-volt cathode in a Li cell. The 4 V material is the spinel crystallographic modification of $LiMn_2O_4$. The cycling data for a 4 V $Li/LiMn_2O_4$ cell is depicted in Fig. 5. The cell has yielded 56 cycles. Subsequently, it failed by what appears to be an internal short (*vide infra*).

The energy densities of the $Li/LiMn_2O_4$ cells are presented in Table 4. With optimization of the thickness of the electrolyte and the composition of the composite cathode, and with improvement of cell packaging, $Li/LiMn_2O_4$ solid-state cells with specific energies of greater than 100 W h kg^{-1} and energy densities of greater than 250 W h l^{-1} are possible.

Solid-state lithium-ion batteries

Lithium-ion batteries consist of Li inserting solid-state anodes such as transition metal oxides [7], Li alloys [7] and carbon [8, 9]. They are Li batteries without metallic Li as the anode. In these, Li ions shuttle between the interstitial sites of the cathode as well as the anode with charge neutralization accomplished by the electrons which are simultaneously transported along the external circuit. Among the perceived advantages of these batteries are: little or no safety hazards because of the absence of metallic Li, high anode cycling efficiency as the anode reactions do not involve plating and stripping of metallic Li, and fast anode reaction kinetics due to the absence of the passivation phenomenon. Carbon anodes composed of disordered graphite or petroleum coke have shown excellent rechargeability in $C/LiCoO_2$ cells utilizing liquid electrolytes [9].

The cycling behavior of a $C/LiNiO_2$ cell with PAN–EC–PC–$LiN(SO_2CF_3)_2$ as the solid polymer electrolyte is shown in Figs. 6(a) and 6(b). The *C*/2 rate corresponds to a current density of 0.25 mA cm^{-2}. The charge/discharge behavior of the $C/LiNiO_2$ cell can be described by:

$$C_6 + LiNiO_2 \rightleftharpoons Li_{0.6}C_6 + Li_{0.4}NiO_2 \quad (4)$$

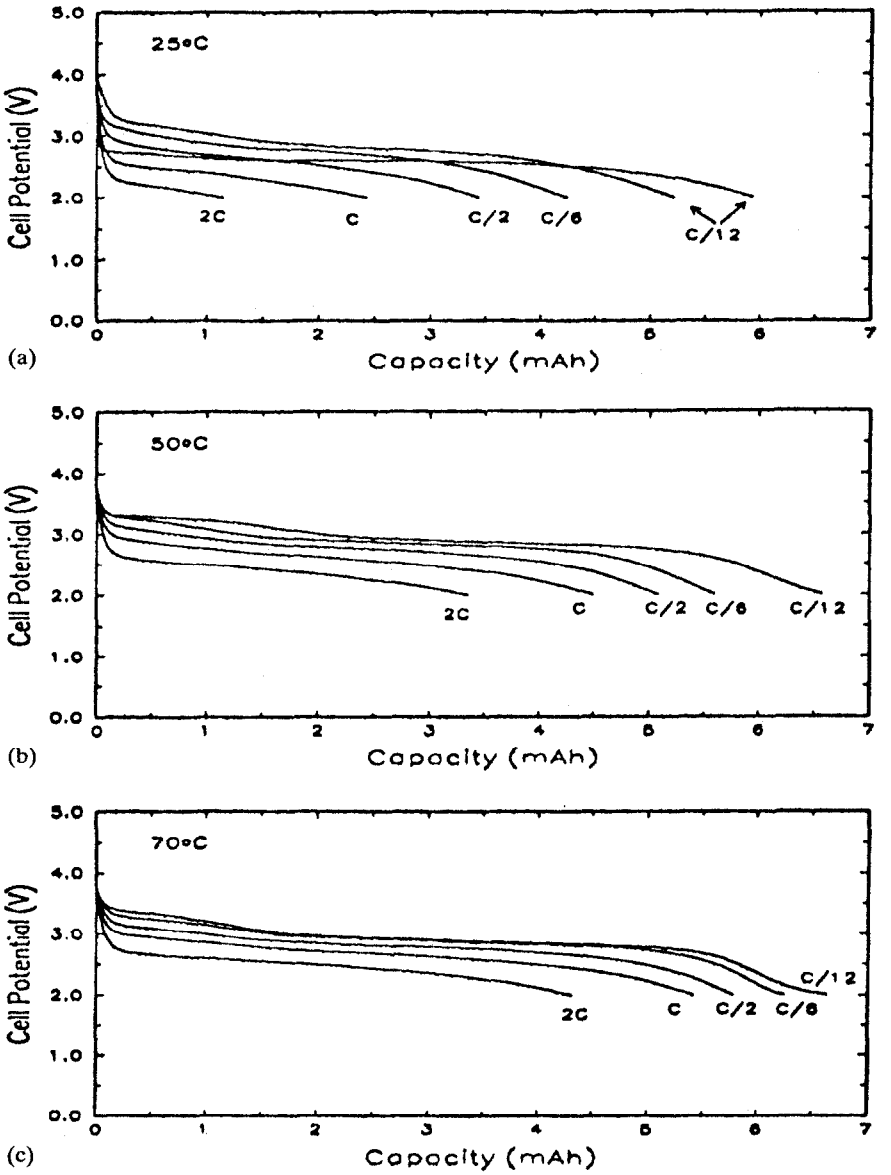

Fig. 3. The capacity–rate behavior of a Li/PAN–EC–PC–$LiAsF_6$/$LiMn_2O_4$ cell at (a) 25 °C, (b) 50 °C, and (c) 70 °C. All charges were at $C/12$ (0.05 mA cm^{-2}).

The cell has a mid-discharge voltage of about 3.0 V, and a quasi-theoretical energy density 1220 W h l^{-1} and a specific energy of 337 W h kg^{-1}. The first discharge in Fig. 6(a) followed an initial charge of the C/SPE/$LiNiO_2$ cell to 3.8 V. This is because carbon anode batteries are assembled in the discharged state and they are activated by charging first, i.e., 'the formation charge'. The efficiency of the first discharge to this 'formation charge' was about 90%. This behavior is reminiscent of the capacity

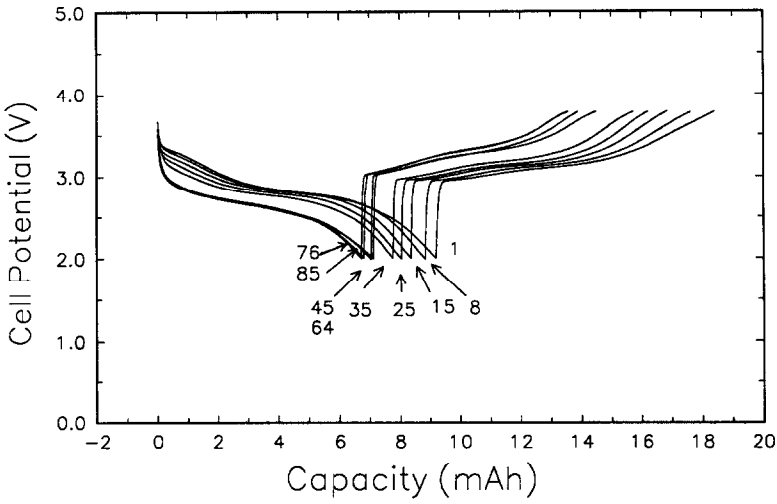

Fig. 4. Cycling curves for a Li/PAN–EC–PC–$LiAsF_6$/$LiMn_2O_4$ cell at room temperature; discharge is at $C/10$ and charge is at $C/20$.

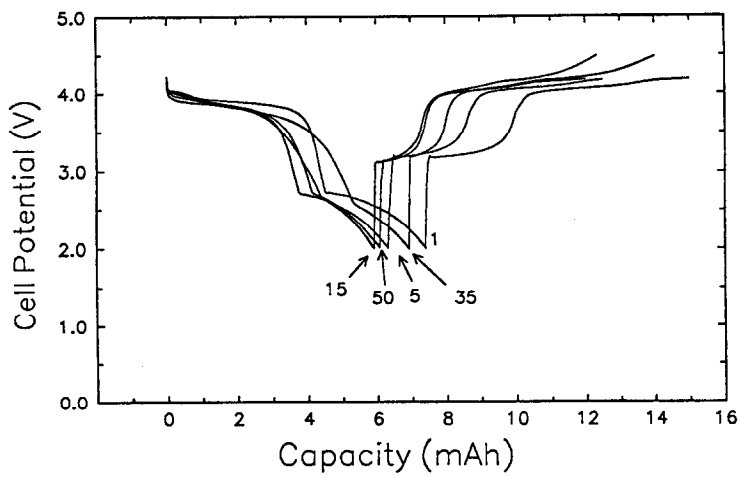

Fig. 5. Cycling curves for a Li/PAN–EC–PC–$LiAsF_6$/spinel $LiMn_2O_4$ cell at room temperature, discharge is at $C/10$ and charge is at $C/20$.

loss reported under similar conditions for the liquid electrolyte-based C/$LiNiO_2$ cell. The coulombic efficiency, however, of each charge/discharge cycle from the second to the 120th cycle was close to 100%. The gradual loss in capacity with cycling reflects a slow increase in the impedance of the cell (*vide infra*). The C/$LiNiO_2$ cell was capable of high rate pulse discharges. This is depicted in Figs. 7(a) and 7(b). The fast relaxation of the cell voltage when the current is turned off after a pulse reflects the fast kinetics of both the C anode and the $LiNiO_2$ cathode. Figure 8 displays the

TABLE 4

Energy densities of solid-state cells

System	Specific energy (W h kg^{-1})		Energy density (W h l^{-1})	
	Present small cells	Future large cells	Present small cells	Future large cells
$Li/LiMn_2O_4$ (3 V battery)	80	⩾120	170	⩾250
$Li/LiMn_2O_4$ (4 V battery)	85	⩾125	180	⩾260
$Carbon/LiNiO_2$	60	⩾100	150	⩾220

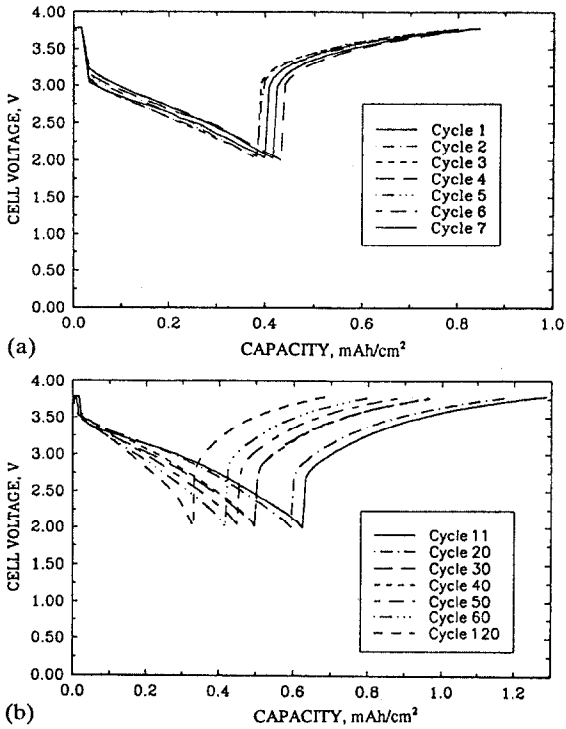

Fig. 6. (a) Cycling behavior of a carbon/PAN–EC–PC–$LiN(SO_2CF_3)_2/LiNiO_2$ cell at the $C/2$ rate, the initial charge performed to activate the cell is not shown; (b) cycles of the carbon/$LiNiO_2$ cell in Fig. 6(a) at the $C/4$ rate from the 11th cycle onwards.

discharge of a bipolar $C/LiNiO_2$ cell, in the pulse mode, at 2 mA cm^{-2}. The cell was pulsed more than 750 times. The practical energy density estimated for a $C/LiNiO_2$ cell is given in Table 4.

The charge/discharge behavior of a carbon/PAN–electrolyte/$LiCoO_2$ cell is presented in Fig. 9. The cell reactions can be described by:

$$C_6 + LiCoO_2 \rightleftharpoons Li_{0.6}C_6 + Li_{0.4}CoO_2 \quad (5)$$

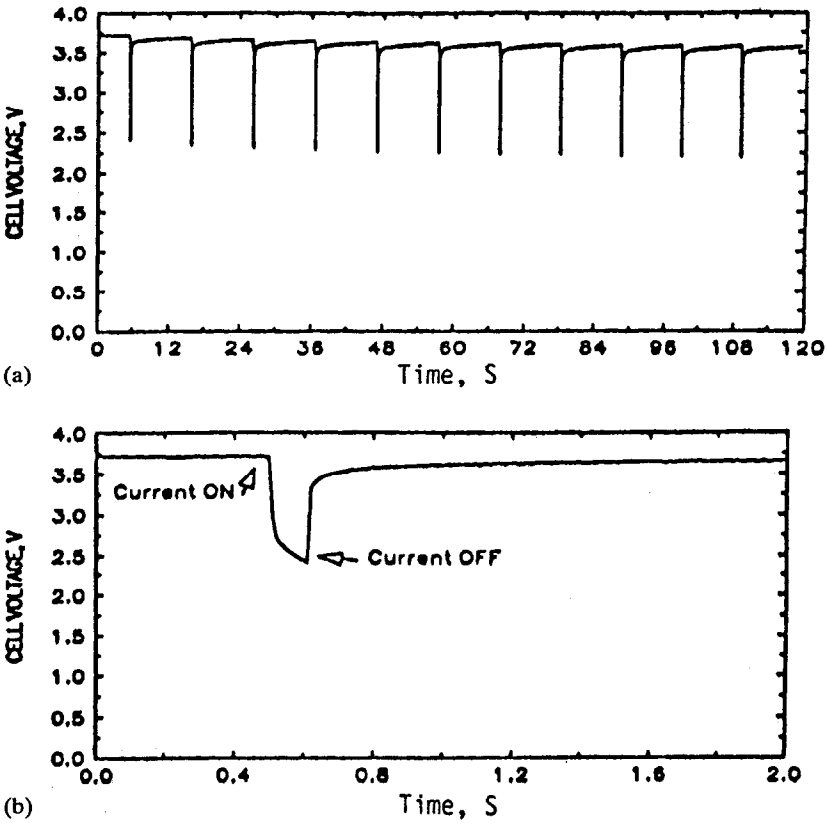

Fig. 7. (a) Typical discharge plots of the carbon/$LiNiO_2$ cell when pulsed at 20 mA cm^{-2} for 0.1 s with 10 s rest period; (b) expanded view of a single pulse. Current: 20 mA cm^{-2}, pulse width: 0.1 s and rest period: 10 s.

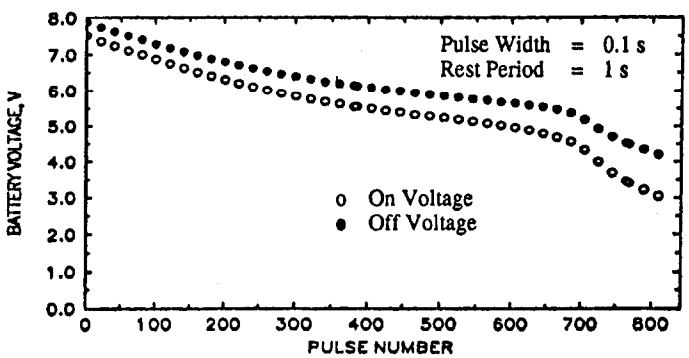

Fig. 8. The 'on' and 'off' voltages of a carbon/PAN–EC–PC–$LiN(SO_2CF_3)_2$/$LiNiO_2$ bipolar battery when pulsed at 2 mA cm^{-2} for 0.1 s with a rest period of 1 s between pulses.

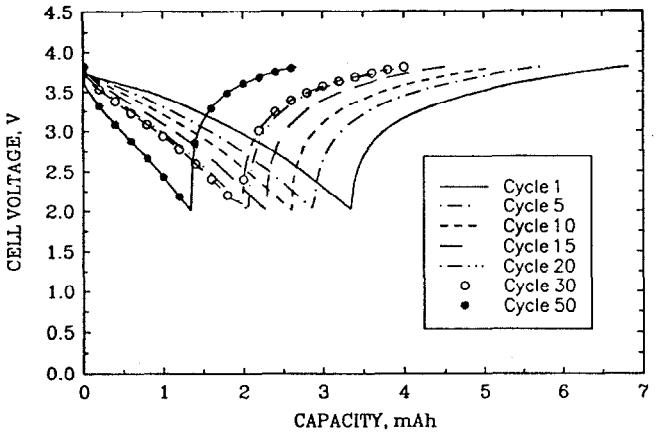

Fig. 9. Cycling behavior of a carbon/PAN-based electrolyte/$LiCoO_2$ cell at room temperature; discharge at 0.12 mA cm^{-2}, charge at 0.12 mA cm^{-2}.

The mid-discharge voltage of the cell is about 3.2 V. It has a quasi-theoretical energy density of 1290 W h l^{-1} and a specific energy of 365 W h kg^{-1}.

Factors limiting cycle life of polymer-electrolyte batteries

The availability of only a limited amount of data at present prevents us from drawing firm conclusions regarding the cycle life failure mechanisms of polymer-electrolyte batteries. However, some of our observations may be useful to the readers. We have found that the capacity of both the Li anode and the Li ion solid-state cells declines with cycling. A close examination of the cycle-life profiles of the Li anode cells revealed that only a very small amount of capacity loss occurred in the first ten or so cycles. Subsequently, a steady but slow rate of decline took place. In an attempt to understand this behavior, the impedance of the Li/SPE/$LiMn_2O_4$ cell shown in Fig. 4 was monitored during the course of cycling. The data are presented in Fig. 10. The semicircle results from a parallel combination of the resistance and capacitance of the Li/polymer-electrolyte interphase. Consequently, the diameter of the semicircle, i.e., the distance between the two points where the semicircle meets the real axis, provides a measure of the resistance of the Li/polymer-electrolyte interphase. There is a significant reduction in the cell's impedance after two cycles. It decreased still further, at a lower rate, until about the 10th cycle. The impedance changed little between the 10th and the 30th cycle. Subsequently, it slowly increased. The rapid decrease in the cell's impedance in the first few cycles is probably related to the electrochemical stripping of the native passivation film on the Li surface and the associated reduction in the resistance of the Li/polymer-electrolyte interphase. The source of the impedance increases later on in cycling is not well understood at this time. It may be the result of accumulation of reaction products at the Li/polymer-electrolyte interphase. Since this cell is still cycling the manner in which the impedance relates to the failure of the cell cannot be reported at this time.

Many a time Li anode cells developed high impedance 'shorts' on charge. Cycles showing these shorts are characterized by a significantly more charge input than the preceding discharge. The cell also shows a difficulty to reach the charge voltage cutoff. This is shown in Fig. 11. We have found a similar behavior for a Li/MEEP–$(LiX)_n$/

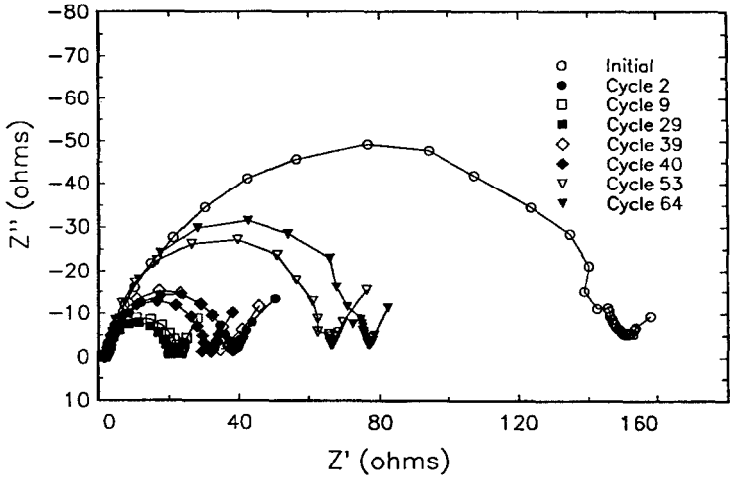

Fig. 10. Impedance history for the Li/polymer-electrolyte/$Li_xMn_2O_4$ cell shown in Fig. 4; frequency range: 100 kHz–0.5 Hz.

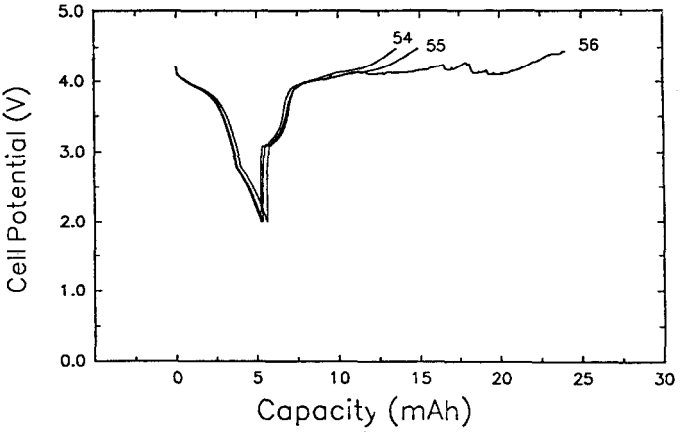

Fig. 11. Failure of a Li/polymer-electrolyte/$Li_xMn_2O_4$ cell by shorting. This is the same cell as in Fig. 5.

TiS_2 cycled at 50 °C [6]. Apparently, the shorting on charge failure mode traditionally identified with liquid electrolyte-based rechargeable Li batteries can be encountered in polymer-electrolyte Li batteries also.

The impedance data recorded as a function of cycle number for the C/$LiNiO_2$ cell displayed in Fig. 6 seemed to indicate that the gradual decrease in capacity with cycling resulted from the rising internal impedance. The reduction of the electrolyte on the carbon anode may be a source of this.

Conclusions

A critical assessment of the structure–property relationship of polymer electrolytes has led to the development of electrolytes with room temperature conductivities of

about $2 \times 10^{-3}\ \Omega^{-1}\ cm^{-1}$. Lithium and Li ion anode batteries employing these electrolytes have shown performance capabilities reminiscent of their liquid electrolyte counterparts.

Acknowledgement

This work was carried out with financial support from the Department of Energy under Grant DEFG01-90ER81078 and by the Strategic Defense Initiative Organization under Contract F29601-91-C-0067 monitored by the Air Force.

References

1 K. M. Abraham, Highly conductive polymer electrolytes, in B. Scrosati (ed.), *Applications of Electroactive Polymers,* Chapman and Hall, London, Ch. 3, in press.
2 K. M. Abraham and M. Alamgir, *Chem. Mater., 3* (1991) 339.
3 K. M. Abraham and M. Alamgir, *J. Electrochem. Soc., 137* (1990) 1657.
4 M. Alamgir, R. D. Moulton and K. M. Abraham, in K. M. Abraham and M. Salomon (eds.), *Primary and Secondary Lithium Batteries,* Proc. Vol. 91–3, The Electrochemical Society, Pennington, NJ, USA, p. 131.
5 R. Koksbang, I. I. Olsen, P. E. Tonder, N. Kundsen, J. S. Lundsgaard and S. Yde-Andersen, *J. Power Sources, 32* (1990) 175.
6 M. Alamgir, R. D. Moulton and K. M. Abraham, *Proc. 34th Int. Power Sources Symp., Cherry Hill, NJ, USA, June 1990,* Institute of Electrical and Electronics Engineers, Inc., IEEE, New York, 1990, p. 167.
7 K. M. Abraham, D. M. Pasquariello and E. B. Willstaedt, *J. Electrochem. Soc., 137* (1990) 743.
8 R. Fong, U. Von Sacken and J. R. Dahn, *J. Electrochem. Soc., 137* (1990) 2009.
9 T. Nagaura, A Li ion rechargeable battery, *4th Int. Rechargeable Battery Seminar, Deerfield Beach, FL, USA, Mar. 1990.*